CONCRETE LIBRARY OF JSCE NO. 22, DECEMBER 1993

TENSION SOFTENING DIAGRAM AND FLEXURAL FAILURE BEHAVIOR OF STEEL FIBER REINFORCED CONCRETE

(Reprint from Proceedings of JSCE, No.460/V-18, Feb. 1993)

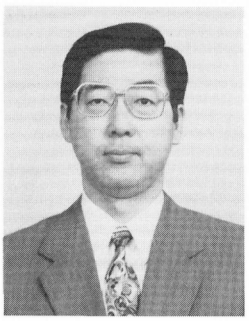
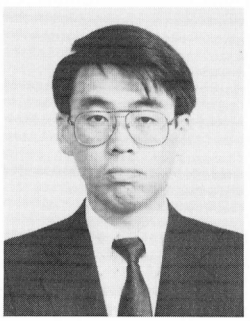
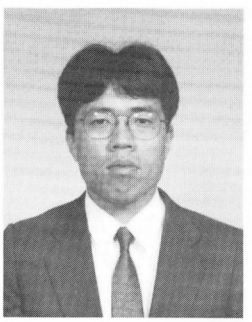


Keitetsu ROKUGO　　Yuichi UCHIDA　　Hidenori KATO　　Wataru KOYANAGI

SYNOPSIS

Load-deflection curves for various sizes of steel fiber reinforced concrete (SFRC, 1% fiber by volume) beams are examined both experimentally and analytically. Tension softening diagrams for SFRC are determined through our modified J-integral-based method. Load-deflection curves for SFRC beams (heights 100, 200, and 400 mm) are simulated and the numerical results are in good accordance with the test results. There are two peaks in the load-deflection curves for SFRC beams. The second peak becomes higher than the first as the size of the specimen increases. It is seen from numerical results that the first peak of SFRC beams depends on the matrix resistance and that the second peak depends on the resistance due to fiber reinforcement. A size effect is recognized on flexural strength of SFRC.

Keywords: fiber reinforced concrete, fracture mechanics, tension softening, flexural strength

K. Rokugo is a professor of the Civil Engineering Department of Gifu University, Gifu, Japan. He received his Doctor of Engineering Degree in 1980 from Kyoto University. His research work covers the failure behavior of concrete and reinforced concrete members. He is a member of JSCE, JCI, ACI, RILEM, and CEB.

Y. Uchida is an assistant of the Civil Engineering Department of Gifu University. He received his Master of Engineering Degree from Gifu University in 1983. His current research interests include numerical analysis and the fracture mechanics of concrete. He is a member of JSCE, JCI, and ACI.

H. Kato is a civil engineer for Ohbayashi Corporation, Tokyo, Japan. He received his Master of Engineering Degree in 1992 from Gifu University, where this investigation was carried out. He is a member of JSCE and JCI.

W. Koyanagi is a professor of the Civil Engineering Department of Gifu University. He received his Doctor of Engineering Degree in 1977 from Kyoto University. His research interests cover the design methods of concrete structures and the applications of new building materials. He is a member of JSCE, JSMS, JCI, and ACI.

1. INTRODUCTION

Steel fiber reinforced concrete (SFRC) has various outstanding properties and is widely used in the field of construction, particularly for tunnel linings, pavement, shotcrete, etc. The properties of SFRC are generally evaluated with strength and toughness in flexure and compression [1]. However, these parameters are not yet sufficient. The fracture properties of SFRC need to be investigated in more detail so as to establish a structural design method for SFRC as precise as that for ordinary concrete.

It is known that the use of numerical analysis with a tension softening diagram (relationship between crack width and transmitted tensile stress in cracked region) is an effective way to discuss the size effect on flexural strength and the flexural failure behavior of concrete [2, 3]. Hillerborg et al. [4] were first to investigate the size effect on flexural strength of concrete. The authors [5] have proposed an equation for evaluating the size-dependent flexural strength of concrete. Li et al. [6] proposed a J-integral-based method for determining tension softening diagrams from bending tests on notched beams and applied the method to SFRC, aramid fiber reinforced concrete, etc. The authors then proposed the modified J-integral-based method [7].

This paper deals with the tension softening diagram and the size effect on the flexural strength of SFRC. Load-deflection curves of SFRC beams in various sizes are examined both experimentally and analytically.

2. EXPERIMENTAL PROCEDURE

Bending tests on various sizes (beam height) of SFRC beams were carried out to investigate their flexural strength and flexural failure behavior. Detailed information about the bending tests is given elsewhere [8]. Bending tests on SFRC notched beams were also performed to determine the fracture energy and the tension softening diagram.

(1) Steel Fiber Reinforced Concrete (SFRC)

Ready mixed concrete was used to cast the specimens. The base concrete conformed to JIS A 5308, with a proof compressive strength of 350 kgf/cm^2 (34 MPa) and a slump value of 15

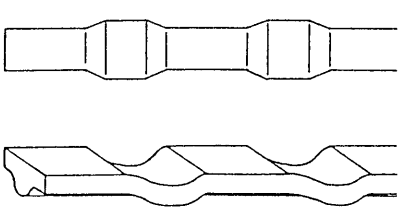

Fig. 1 Shape of steel fiber

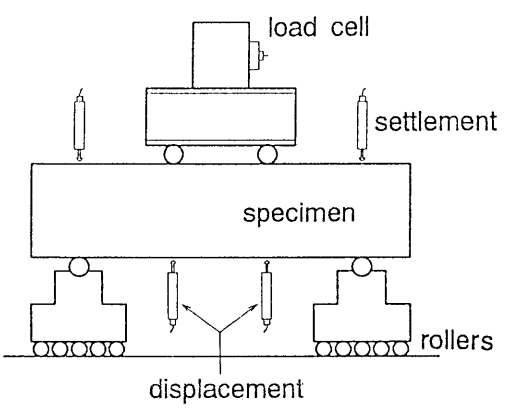

Fig. 2 Third-point bending test on beam

Table 1 Properties of SFRC

Type of concrete	Strength (MPa)			Young's modulus (GPa)	Fracture energy (kN/m)
	Comp.	Tension	Flexure		
SF1	38.2	3.05	5.05	31	3.4
F1	47.4	3.72	6.46	25	4.4
F2	47.0	3.95	8.42	29	8.3

cm. The maximum size of coarse aggregate was 15 mm and the air content was 4%. Indented steel fibers (ø0.6x30 mm) as shown in Fig. 1 were adopted. The volume content of fiber was 1.0%. The slump value of the SFRC was about 3 cm. Strength values for SFRC (SF1) were obtained by standard tests and are tabulated in Table 1. The compressive strength and the Young's modulus were 38.2 MPa and 31 GPa, respectively (specimen size: ø100x200 mm). The splitting tensile strength was 3.05 MPa (specimen size: ø150x150 mm) and the flexural strength was 5.05 MPa (specimen size: 100x100x400 mm).

(2) Loading Tests on Beams in Various Sizes

Four sizes of beam specimens were used. All specimens had a square cross section, and the dimensions (height of the section) were 50, 100, 200, and 400 mm. These specimens are denoted S5, S10, S20, and S40. The specimen length was four times the height and the loaded span was three times the height. The third-point loading tests were carried out. The load was applied to specimens perpendicular to the casting direction. The method of loading and the measuring system is shown in Fig. 2. More than four specimens were provided for each test condition. The relationship between load and deflection at each loading point was measured, except in the case of S5, where only the maximum load was measured.

(3) Loading Tests on Notched Beams

In order to obtain the fracture energy, G_F, of SFRC, three-point bending tests on notched beam specimens were carried out in line with the RILEM recommendation [9]. The specimen size was 100x100x840 mm, the notch depth 50 mm and the span 800 mm. Five specimens were used in this test. The setup of the loading and the measuring system is illustrated in Fig. 3.

The tension softening diagram for SFRC was determined from the relationship among measured

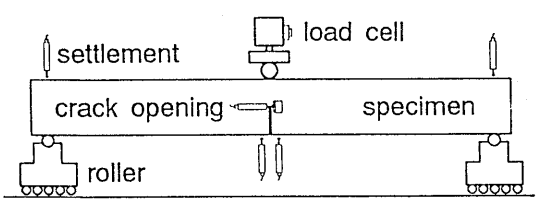

Fig. 3 Three-point bending test on notched beam

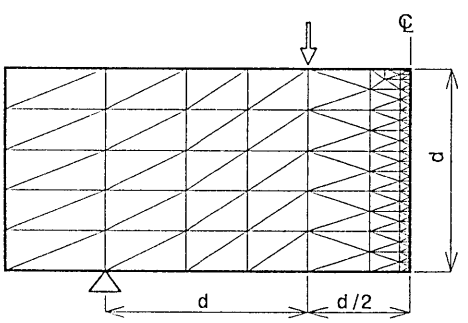

Fig. 4 Finite element mesh

load, deflection at loading points, and crack width at the notch tip (COD) using the modified J-integral-based method [7], a method originating with Li's J-integral-based method [6]. Li's method requires data from two beam specimens with slightly different notch depths, whereas the modified method requires data from only a single specimen to determine one tension softening diagram.

3. FINITE ELEMENT ANALYSIS

In finite element analysis, a fictitious crack model was introduced at the center of the specimen. The growth of the crack was modeled so that each node separated in turn and equivalent nodal forces were transmitted through the nodes. The forces were derived from the tension softening diagram. The FE mesh adopted for this analysis is shown in Fig. 4. Only one half of the specimen was modeled because of its symmetry. The crack was assumed to begin at the tension face and develop straight upwards at the center of the specimen. The material properties given in Table 1 were assumed in the analysis.

4. FLEXURAL STRENGTH AND FLEXURAL LOAD-DEFLECTION CURVES

Measured load-deflection curves for S10, S20, and S40 are shown in Fig. 5(a)-(c). Two peaks were observed for large specimens (S20 and S40). The values of the first and second peak loads, P_1 and P_2, are given in Table 2. For a small specimen (S10), there was only one peak, just as with normal concrete. In the case of S20, the first peak load, P_1, was higher than the second peak load, P_2. Conversely in the case of S40, P_2 was higher than P_1. Only one crack

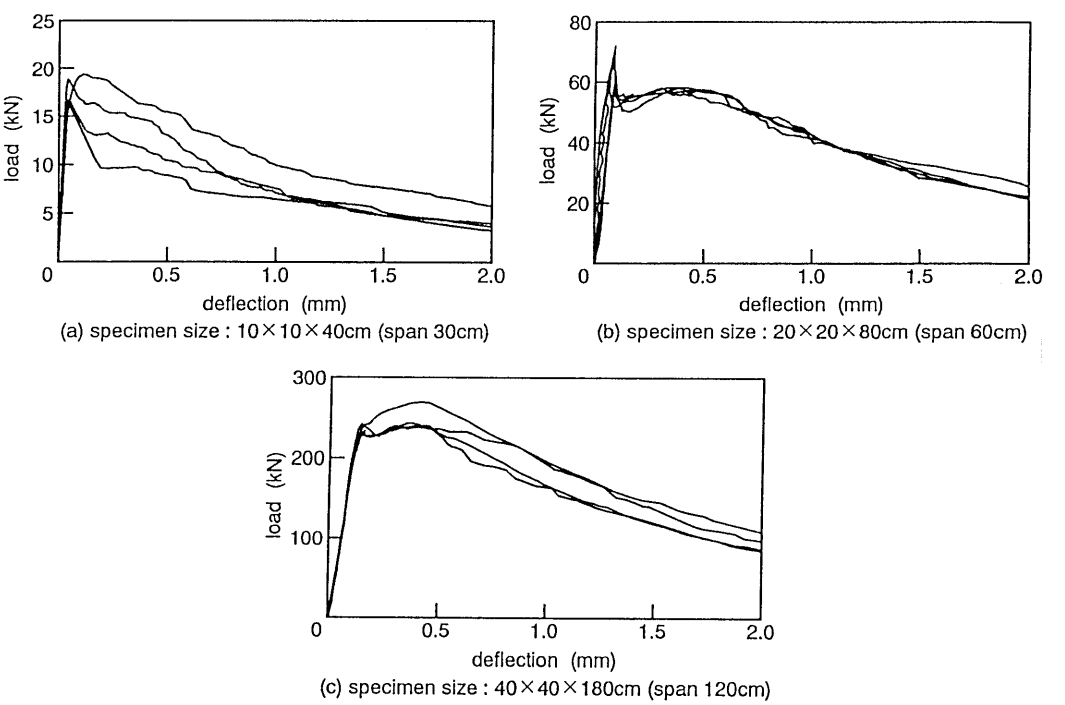

Fig. 5 Measured load-deflection curves of beams

Table 2 Results of tests and analysis

Specimen	Specimen size: width, height, span (mm)	Results of tests				Results of analysis					
		Peak load (kN)		Flex. str. (MPa)		Peak load (kN)		Flex. str. (MPa)		Crack width at peak (mm)	
		P_1	P_2	σ_{b1}	σ_{b2}	P_1	P_2	σ_{b1}	σ_{b2}	COD_1	COD_2
S5	50×50×150	5.1	–	5.91	–	4.7	–	5.69	–	0.023	–
S10	100×100×300	17.2	–	5.05	–	16.9	–	5.06	–	0.050	–
S20	200×200×600	63.6	57.9	4.67	4.26	60.7	58.9	4.55	4.42	0.073	0.566
S40	400×400×1200	236.	248.	4.41	46.5	216.	227.	4.05	4.24	0.084	0.609

was visible in each specimen.

Nominal flexural strengths corresponding to the averaged values of P_1 and P_2 are denoted σ_{b1} and σ_{b2}, respectively, and are given in Table 2 and Fig. 6. The nominal flexural strength was calculated from the peak load divided by its sectional modulus, taking into account the effect of the specimen's own weight. As seen in Fig. 6, σ_{b1} decreases with increasing specimen height and the so-called "size effect" was observed just as in the case of normal concrete. On the other hand, σ_{b2} increases slightly as the specimen height increases from 200 to 400 mm.

5. FRACTURE ENERGY AND TENSION SOFTENING DIAGRAM

(1) Fracture Energy

The fracture energy, G_F, obtained from the load-deflection curves of notched beams by the RILEM method [9] was an average of 3.4 kN/m. When the RILEM method is applied to SFRC, G_F includes not only the fracture energy of the tensile cracking zone, but also a certain amount of energy of the compressive zone.

(2) Tension Softening Diagram

The SFRC tension softening diagram was obtained using the modified J-integral-based method and is shown in Fig. 7. We hereafter refer to this diagram as the J-curve. Immediately after the softening initiation point (tensile strength failure point), the transmitted stress decreases suddenly with increasing crack width. When the crack width reaches about 0.03 mm, the transmitted stress gradually rises because the reinforcing effect of the steel fibers comes into play.

The modified J-integral-based method can be combined with the RILEM method to determine G_F. However, neither the stress at the softening initiation point (tensile strength failure point) nor the complete crack width (at which the transmitted stress vanishes) in the tail part of the tension softening diagram can be determined exactly. The tensile strength as determined through splitting tests is taken to be the stress at the softening initiation point and the complete crack width is determined so that the area under the diagram coincides with G_F.

The load-deflection curve for the notched beam was numerically simulated using the J-curve. The result is shown in Fig. 8 together with the load-deflection curve obtained experimentally. The numerical result correlates well with to the experimental results, except for the magnitude

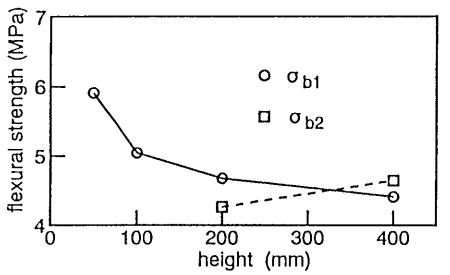

Fig. 6 Flexural strength and beam height (experiment)

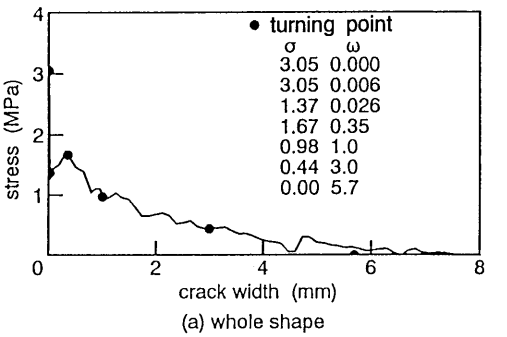

(a) whole shape

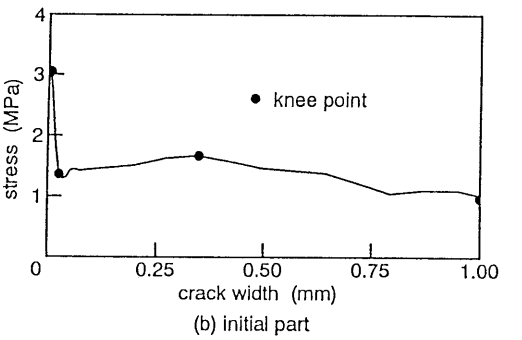

(b) initial part

Fig. 7 Tension softening diagram of SFRC (J-curve)

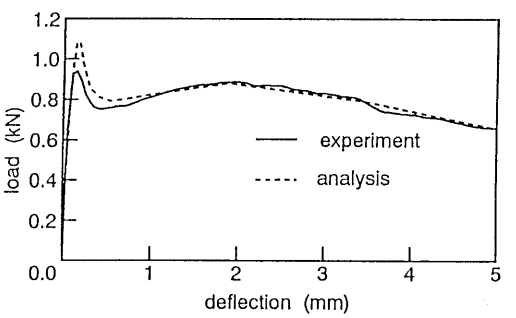

Fig. 8 Load-deflection curve of notched beam

of the first peak load. Load-deflection curves for the specimens of various sizes (heights) were calculated using J-curve, and these are illustrated in Fig. 9. These curves also coincide fairly well with the experimental results and they show the two peaks. In the analysis, the J-curve was expressed as a set of short straight lines. The stress and crack width at each turning point on the line are given in Fig. 7.

(3) Improved Model of Tension Softening Diagram

The tension softening diagram as determined through the modified J-integral-based method is considered to be only an approximation. The SFRC J-curve can be improved further so as to obtain better numerical results. This improved tension softening diagram is defined by a set of five straight lines with the same G_F, as shown in Fig. 10. The diagram is named model-I. The area under the model-I line between the turning points A and B is greater than that under the J-curve. The crack width at point B is 0.1 mm.

Simulated load-deflection diagrams for each size of specimen based on model-I are shown in Fig. 9. They agree rather better with the experimental results than those based on the J-curve. In particular, the relationship between the two peak loads, P_1 and P_2, for various specimen sizes is correctly estimated.

The best way to measure tension softening diagrams for concrete is to carry out direct tension tests. If such direct tension tests can not be performed, it is recommended that an approximation of the diagrams be determined from three-point bending tests on notched beams

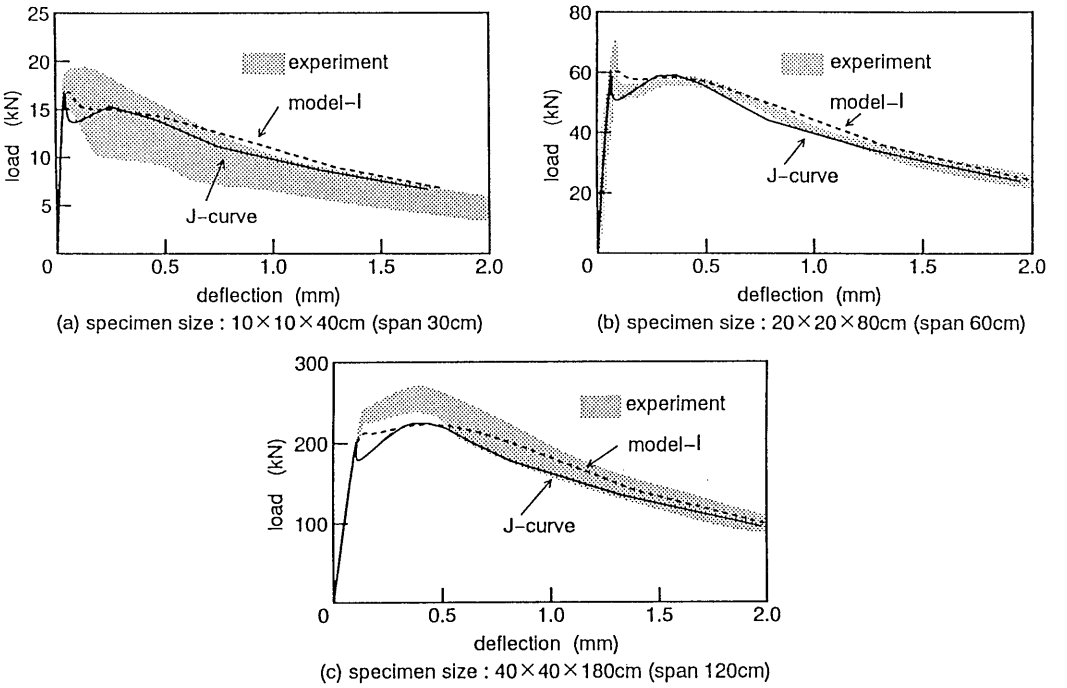

Fig. 9 Simulated load-deflection curves of beams

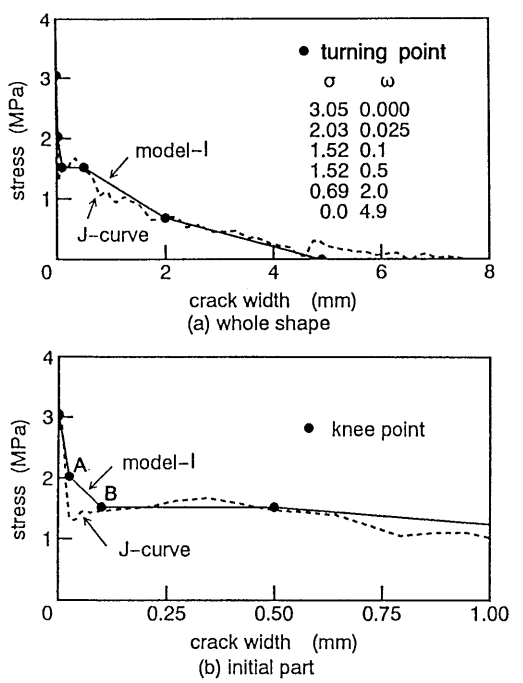

Fig. 10 Improved model of tension softening diagram (Model-I)

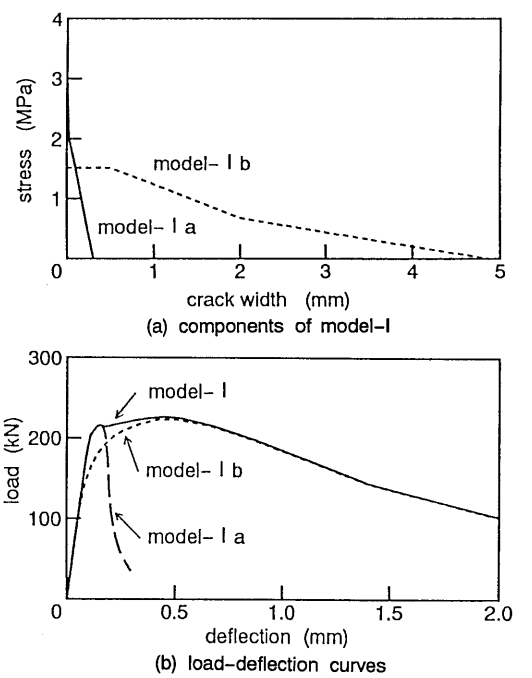

Fig. 11 Components of tension softening diagram and load-deflection curves

by the modified J-integral method. The shape of the diagrams can be improved through numerical analysis.

6. PEAK LOAD OF BEAMS IN BENDING

With a beam height of 200 or 400 mm, there are two peaks in the load-deflection curves obtained from both experiments and from numerical analysis using the model-I. The numerical results for peak loads, P_1 and P_2, as well as for the corresponding crack widths on the underside (tension side), COD_1 and COD_2, are shown in Table 2. COD_1 is smaller than the crack width at point B (0.1 mm), but COD_2 is larger. It is possible that P_1 depends on the resistance of the matrix and P_2 depends on the reinforcing effects of the steel fibers.

Model-I is considered to consist of two portions, model-Ia and model-Ib, as shown in Fig. 11(a). The load-deflection curves derived from model-I and its components (model-Ia and model-Ib) are shown in Fig. 11(b). The peak load in the curve derived from model-Ia coincides with P_1, and that derived from model-Ib is close to P_2. Therefore, the flexural strength σ_{b1} derived from P_1 represents the flexural strength of the matrix, and σ_{b2} from P_2 relates to the effects of the fiber reinforcement. For small specimens (S5, S10, and S20) where $P_1>P_2$, fiber reinforcement does not contribute to the maximum load. In the case of the SFRC in this study, fiber reinforcement has an effect on the maximum load only when the specimens are large (S40).

7. SIZE EFFECT ON FLEXURAL STRENGTH

The flexural strengths σ_{b1} and σ_{b2} obtained from numerical analysis are included in Table 2. As mentioned before, the flexural strength is calculated from the peak load divided by the sectional modulus, taking account of the effect of the specimen's own weight.

Figure 12 shows the relationship between calculated flexural strength and specimen height, including 600, 800, and 1000 mm specimens (called S60, S80 and S100) beyond the range of the experiments. Model-I was used in the analysis as the tension softening diagram. The calculated results for normal concrete reported by authors [5] are also shown in Fig. 12, where the tensile strength of the concrete was 2.79MPa, the fracture energy G_F was 0.1 kN/m, and the so-called "1/4 model" for the tension softening diagram was adopted. The 1/4 model is

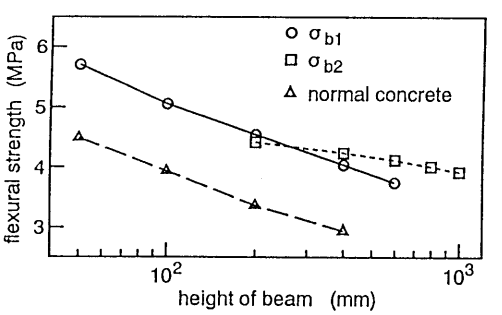

Fig. 12 Flexural strength and beam height (analysis)

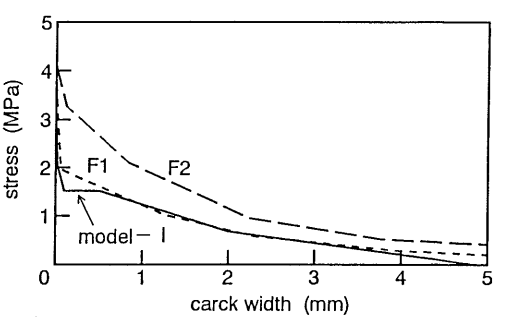

Fig. 13 Three types of tension softening diagram

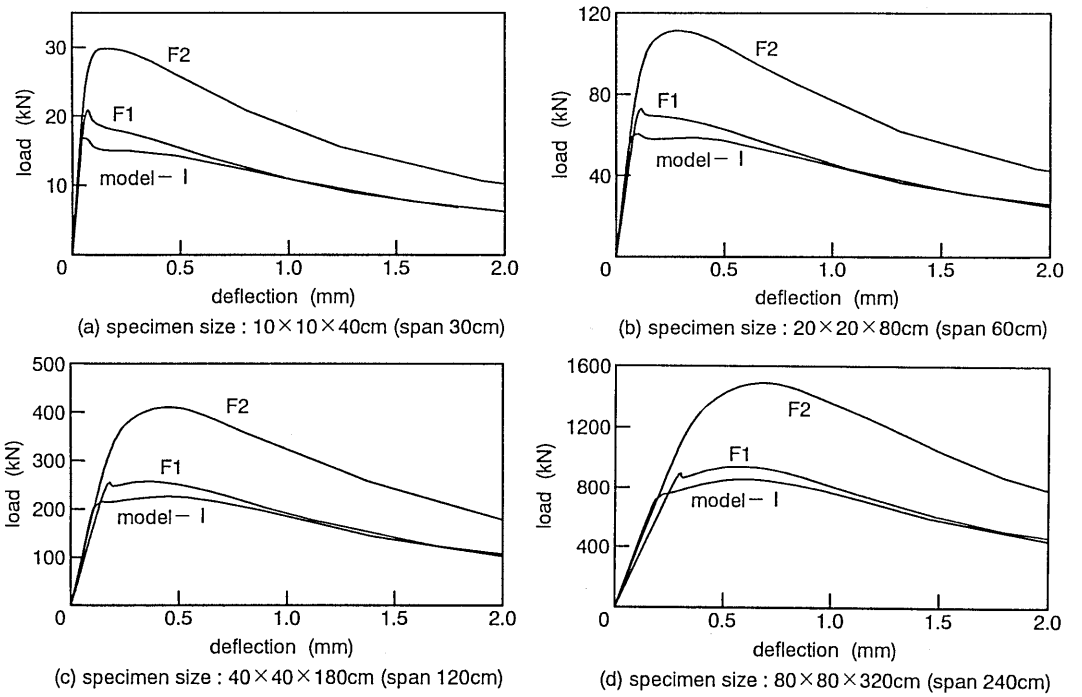

Fig. 14 Effect of tension softening diagram on load–deflection curves

expressed in terms of a bilinear line and the stress at the turning point is 1/4 of the tensile strength. As shown in Fig. 12, the flexural strength of SFRC decreases with the specimen size increases. The gradient of this line for SFRC is almost the same for that of normal concrete, though the strength itself is higher for SFRC than for normal concrete. The gradient of the fall in σ_{b2} with specimen height is smaller than that for σ_{b1}. This means that the size effect becomes smaller when the effect of the steel fiber reinforcement becomes dominant.

8. EFFECT OF MATERIALS ON SHAPE OF LOAD-DEFLECTION CURVES

The effects of the shape of both tension softening diagrams and material properties — such as the fracture energy G_F and Young's modulus E_c — on the load–deflection curves are numerically investigated. The tension softening diagrams shown in Fig. 13 and the material properties given in Table 1 are considered in the analysis. Figure 13 includes not only model–I but also tension softening diagrams for SFRC with 1% and 2% steel fiber (called F1 and F2) [10]. The compressive strength of F1 in the previous study was 25% higher than that of SF1 in this study, and the fracture energy G_F of F1 was 30% greater.

Figure 14 shows simulated load–deflection curves for beams with a square cross section and different heights, namely, 100, 200, 400, and 800 mm. Third-point loading conditions were assumed. The load–deflection curves simulated with the F1 model show a larger peak load than those simulated with model–I. In the case of F2 (SFRC with 2% steel fiber), there is only one peak on the load–deflection curves for all beam sizes. In the case of F1 (SFRC with 1% steel fiber), two peaks appear on the load–deflection curve when the beam height is 400 or 800 mm.

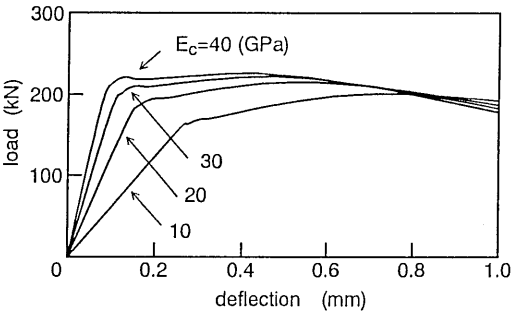

Fig. 15 Effect of Young's modulus on load–deflection curves

Load–deflection curves for beams of height 400 mm are simulated using model–I and various values of Young's modulus (E_c= 10, 20, 30, and 40 GPa). These are shown in Fig. 15. With an increase in Young's modulus, not only does the initial slope of the load–deflection curves increase, but the peak load rises too.

9. CONCLUSIONS

Tension softening diagrams and the size effect on both the flexural strength and load–deflection curves of SFRC beam specimens with 1% steel fiber were investigated both analytically and experimentally.

The tension softening diagram for SFRC (J–curve) was determined by carrying out bending tests on notched beams using the J–integral–based method. The tension softening diagram showed that the effects of fiber reinforcement appear when the crack width reaches 0.03 mm. Simulated load–deflection curves for beams of various sizes were agreed well with the experimental results. Model–I (a further modification to the J–curve) was used as softening diagrams for the FE analysis.

Two peaks were observed in the load–deflection curves for large beams (height: 200 and 400 mm), though only one peak was observed for the small beams (height: 100 mm). The second peak became higher than the first in the case of the largest beams (height: 400 mm). Numerical results indicate that the first peak depends on the strength of the matrix while the second relates to the effects of fiber reinforcement. A size effect on the flexural strength of SFRC was recognized. This effect became smaller in the case of large beams (height: 400 mm), where the effects of the steel fiber reinforcement became dominant.

This work emphasizes the utility of the tension softening diagram as a parameter describing the fracture behavior of SFRC in tension and flexure. It also suggested that a combination of numerical analysis with a tension softening diagram is an effective way to discuss the size effect on the flexural failure behavior of SFRC beams.

ACKNOWLEDGEMENT

The authors acknowledge the financial support for this study given by the Kajima Foundation's Research Grant and by a Grant–in–Aid from the Ministry of Education.

REFERENCES

[1] JCI Committee on FRC, "JCI Standards for Test Methods of Fiber Reinforced Concrete," Japan Concrete Institute, JCI-SF, 68p., 1984.2

[2] JCI Committee on FMC, "Committee Report on Fracture Mechanics of Concrete," Japan Concrete Institute, JCI-C19, 167p., 1990.3 (in Japanese)

[3] Mihashi, H., Shirai, N., and Rokugo, K., "Application of Fracture Mechanics to Concrete Structures," JCI Concrete Journal, Vol.30, No.6, pp.5-17, 1991.6 (in Japanese)

[4] Hillerborg, A., Modeer, M, and Petersson, P.E., "Analysis of Crack Formation and Crack Growth in Concrete by Means of Fracture Mechanics and Finite Elements," Cement and Concrete Research, Vol.6, No.6, pp.773-782, 1976

[5] Uchida, Y., Rokugo, K., and Koyanagi, W., "Application of Fracture Mechanics to Size Effect on Flexural Strength of Concrete," Proc. JSCE, No.442/V-16, pp.101-107, 1992.2 (in Japanese) ／ Concrete Library of JSCE, No.20, pp.87-97, 1992.12

[6] Li, V.C. and Ward, R.J., "A Novel Testing Technique for Post-Peak Tensile behavior of Cementitious Materials," Fracture Toughness and Fracture Energy, Balkema, pp.183-195, 1989

[7] Uchida, Y., Rokugo, K., and Koyanagi, W., "Determination of Tension Softening Diagrams of Concrete by Means of Bending Tests," Proc. JSCE, No.426/V-14, pp.203-212, 1991.2 (in Japanese) ／ Concrete Library of JSCE, No.18, pp.171-184, 1991.12

[8] Rokugo, K., Uchida, Y., and Koyanagi, W., "Size Effects on Modulus of Rupture of Steel Fiber Reinforced Concrete," CAJ Proc. of Cement & Concrete, No.45, pp.482-487, 1992 (in Japanese)

[9] RILEM Draft Recommendation (50-FMC), "Determination of the Fracture Energy of Mortar and Concrete by Means of Three-Point Bend Tests on Notched Beams," Materials and Structures, Vol.18, No.106, pp.285-290, 1985

[10] Rokugo, K., Iwasa, H., Suzuki, Y., and Koyanagi, W., "Fracture Mechanics Parameters of Different Kinds of Concrete," Proc. of JCI, Vol.11, No.1, pp.247-252, 1989 (in Japanese)